Journal of Neuropathology and Experimental Neurology

Vol. 60, No. 7
July, 2001
pp. 686–695

Expression and Activities of Aldo-Keto Oxidoreductases in Alzheimer Disease

MATTHEW J. PICKLO, SR., PHD, SANDRA J. OLSON, MS, WILLIAM R. MARKESBERY, MD, AND THOMAS J. MONTINE, MD, PHD

Abstract. A reactive intermediate generated by lipid peroxidation, 4-hydroxy-2-nonenal (HNE), has received considerable attention as a potential effector of oxidative damage and Aβ peptide-mediated neurotoxicity in Alzheimer disease (AD). However, little is known about aldo-keto oxidoreductases, a group of enzymes that constitute a major detoxifying pathway for HNE and related reactive aldehydes in human brain. We have determined the regional, cellular, and class distribution in human brain of the 4 major aldo-keto oxidoreductases that detoxify HNE: aldehyde dehydrogenase (ALDH); aldose reductase; aldehyde reductase; and alcohol dehydrogenase (ADH). Of these 4 enzymes, only ALDH and aldose reductase were expressed in cerebral cortex, hippocampus, basal ganglia, and midbrain; all 4 enzymes were present in cerebellum. In cerebrum and hippocampus, aldose reductase was localized to pyramidal neurons and mitochondrial class 2 ALDH was localized to glia and senile plaques. ALDH, but not aldose reductase, activity was significantly increased in temporal cortex from patients with AD compared to age-matched controls. These results suggest that in brain regions involved in AD, neurons and glia utilize different mechanisms to detoxify HNE, and that increased ALDH activity is a protective response of cerebral cortex to AD.

Key Words: Aldehyde dehydrogenase; Aldose reductase; Alzheimer disease; 4-Hydroxynonenal.

INTRODUCTION

4-Hydroxy-*trans*-2-nonenal (HNE) and related carbonyls, such as acrolein, are reactive intermediates generated from oxidative damage to polyunsaturated fatty acids (1, 2). These α,β unsaturated aldehydes are electrophilic compounds that alkylate nucleophilic groups located on proteins, nucleic acids, and aminophospholipids (2–5). HNE-protein adduct and acrolein-protein adduct immunoreactivity, brain tissue levels of HNE, and cerebrospinal fluid levels of HNE are elevated in patients with Alzheimer disease (AD), Parkinson disease, and amyotrophic lateral sclerosis (6–13). Several in vitro and cell culture experiments have suggested that these reactive carbonyls may contribute to neurodegeneration by a number of mechanisms (14–19). HNE directly inhibits respiration at the level of complex III activity in isolated rat brain mitochondria (14). Disruption of the cytoskeleton and direct modification of tubulin has been demonstrated in Neuro2A cells (15). Cell culture experiments using primary hippocampal neurons demonstrate that HNE treatment depletes cellular glutathione, induces de novo lipid peroxidation, and inhibits mitochondrial function (19). Synaptosomal studies indicate that HNE forms adducts upon and inhibits the glutamate transporter (17). Alterations in these parameters are associated with neurodegenerative disease. Indeed, based on experiments using neuronal cultures, HNE has been proposed as one of the principal effectors of Aβ peptide-mediated neurodegeneration (20, 21).

Analogous to superoxide dismutases, glutathione peroxidases, and catalase that detoxify reactive oxygen species, cytoprotective enzymes have evolved that catalyze the detoxification of reactive aldehydes. Two major detoxification pathways exist for HNE and acrolein. First is the glutathione pathway in which the electrophile is conjugated to glutathione, primarily through the action of glutathione S-transferases (GSTs) (22, 23). Decreased GST activity has been reported in diseased regions of AD brain, a result that may be interpreted as suggesting limited biological significance of reactive carbonyls in AD, or as suggesting that AD brain has diminished protection from the neurotoxic effects of HNE and related aldehydes (24). The other major metabolic pathway for aldehyde detoxification is oxidation or reduction of the aldehyde to its corresponding acid or alcohol, respectively, by aldo-keto oxidoreductases (25, 26).

Aldehyde oxidation to the corresponding acid is catalyzed by aldehyde dehydrogenases (ALDH; EC 1.2.1.3). Class 1 and class 2 ALDH are NAD+ requiring enzymes that have a low K_M (<10 μM) towards propionaldehyde and that metabolize HNE to its corresponding acid, 4-hydroxy-(2)-nonenoic acid (25, 27). Class 1 ALDH is located within the cytosol and has a pI of 5.1; class 2 ALDH is localized to mitochondria and has a pI of 4.9. In contrast, class 3 ALDH utilizes either NAD^+ or $NADP^+$ as cofactors in vitro, has a high K_M (>2 mM), and does not metabolize HNE (28). ALDH activity and expression have been determined in human brain where only class 2 ALDH mRNA has been detected (27, 29–31). However, the regional and cellular localization of ALDH in human brain,

From the Departments of Pathology (MJP, SJO, TJM) and Pharmacology (TJM), Vanderbilt University Medical Center, Nashville, Tennessee; Sanders-Brown Center on Aging and the Departments of Pathology and Neurology (WRM), University of Kentucky Medical Center, Lexington, Kentucky.

Correspondence to: Matthew J. Picklo, Sr., PhD, Department of Pharmacology, Physiology, and Therapeutics, University of North Dakota School of Medicine and Health Sciences, 501 North Columbia Road, Grand Forks, ND 58203.

This work was supported by grants from the NIH (ES05826, ES10196, AG00774, AG16835, and AG05144) and the Alzheimer's Association (IIRG-98-40).

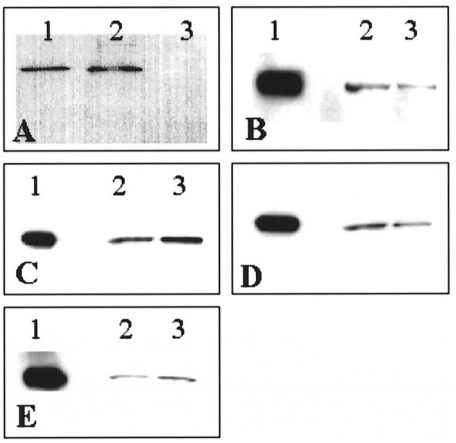

Fig. 1. Characterization of aldo-keto oxidoreductase antisera. A: Anti-ALDH antibodies recognize class 1 and class 2 but not class 3 ALDH. Class 1, 2, or 3 ALDH (100 ng each) were loaded per lane in lanes 1, 2, 3, respectively, electrophoresed, transferred to PVDF membrane, followed by probing with anti-ALDH antibody. B: Low K_M ALDH is present in the frontal cortex and hippocampus. Class 2 ALDH (20 ng) was loaded in lane 1, 10 μg of protein from homogenates of postmortem frontal cortex (lane 2) and hippocampus (lane 3). C: Aldose reductase is present in the frontal cortex and hippocampus. Purified, recombinant, human, aldose reductase (20 ng) was loaded in lane 1, 10 μg of protein from homogenates of postmortem frontal cortex (lane 2) and hippocampus (lane 3). D: Aldehyde reductase is present in the frontal cortex and hippocampus. Purified, recombinant, human, aldehyde reductase (20 ng) was loaded in lane 1, 10 μg of protein from homogenates of postmortem frontal cortex (lane 2) and hippocampus (lane 3). E: Alcohol dehydrogenase is present in the frontal cortex and hippocampus. Purified, human alcohol dehydrogenase (β_1; 20 ng) was loaded in lane 1, 7 μg of protein from homogenates of postmortem frontal cortex (lane 2) and hippocampus (lane 3). The sample of frontal cortex was derived from a patient with AD and the hippocampal sample was from a control individual.

and the activity of this enzyme in AD brain is not known. The potential importance of ALDH activity in AD was underscored recently by the report of an increased risk for AD in Japanese patients who inherited the *ALDH2*2* allele, which encodes a dominant negative inactive form of class 2 ALDH (32).

Aldehyde reduction to the corresponding alcohol is catalyzed by members of the aldo-keto reductase superfamily (AKR), aldehyde reductase (AKR1A1; EC 1.1.1.2), and aldose reductase (AKR1B1; EC 1.1.1.21), as well as by 3 classes of alcohol dehydrogenases (ADH EC 1.1.1.1) (26, 33–35). Aldehyde reductase is approximately 3-fold more active towards HNE than aldose reductase although both metabolize acrolein at the same rate (26). One immunohistochemical survey of human tissue for aldose reductase described immunoreactivity with ''neuronal cells and neuroglial elements'' in cerebrum and with all components of cerebellum except internal granule cells (36). Class 1 and class 2 ADH catalyze reduction of HNE; however, class 3 ADH, a glutathione-dependent formaldehyde dehydrogenase, does not metabolize HNE (33). In human brain, immunoreactivity for class 3 ADH is present in cerebellar Purkinje cells and some pyramidal neurons of the cerebral cortex and hippocampus; however, class 1 ADH shows only vascular immunoreactivity and immunohistochemical analysis for class 2 ADH has not been reported (37). We are not aware of any study that has investigated activity, localization, or genetic associations for these reductases in AD.

The compelling evidence from in vitro and human tissue studies for a pathogenic role for HNE and related aldehydes in AD and the recent genetic association between an inactive isoform of ALDH and AD underscore the potential importance of these cytoprotective enzymes in brain. Therefore, we have determined the regional, cellular, and class distribution in human brain of the 4 major aldo-keto oxidoreductases that detoxify HNE: ALDH, aldose reductase, aldehyde reductase, and ADH. In addition, we tested the hypothesis that altered cellular localization and increased activities of aldo-keto oxidoreductases may occur as a protective response to reactive aldehyde generation in AD.

MATERIALS AND METHODS

Human Brain Tissue

Following appropriate consent, all individuals included in this study had postmortem examinations as part of rapid autopsy programs at the University of Kentucky Alzheimer's Disease Research Center or Vanderbilt University Medical Center. No patient had a postmortem interval (PMI) greater than 3 hours (h). All tissue was kept frozen at −80°C until used. All AD patients were diagnosed with probable AD during life and were shown by neuropathological examination to meet the criteria for definite AD (38). Controls were age- and gender-matched individuals without clinical evidence of dementia or other neurological disease. Each control subject had annual neuropsychological testing with all test scores in the normal range.

Antibodies and Purified Proteins

Anti-ALDH antiserum raised against class 2 enzyme and purified class 1 and class 2 ALDH proteins were the kind gift of Dr. Henry Weiner (Purdue University). Anti-aldose reductase and anti-aldehyde reductase antisera were the kind gift of Dr. John Hayes (University of Dundee) (26). Anti-ADH antiserum recognizing class 1 and class 2 ADH, but not class 3 enzyme, and purified ADH β_1 protein were the kind gift of Dr. Thomas Hurley (Indiana University Medical Center). Recombinant human aldose reductase and aldehyde reductase were expressed in *E. coli* using a pET15b vector encoding human aldose reductase N-terminally fused to 6 histidine residues and a thrombin cleavage site as described by O'Connor et al (26). Expression was induced and protein purified as previously described using Ni-NTA chelating agarose (Qiagen, Valencia, CA) (26). Protein purity was analyzed by SDS-PAGE. Protein was dialyzed extensively into PBS (125 mM NaCl, 10 mM NaH_2PO_4, pH 7.2, 0.1% Triton X-100) prior to use. Protein concentration

TABLE
Immunohistochemical Localization of Aldehyde Dehydrogenase and Aldose Reductase in Human Brain

	Aldehyde Dehydrogenase	Score	Aldose Reductase	Score
Frontal and	Neurons	−	Some Pyramidal neurons	+
Temporal	Glia	++	Glia	−
Cerebral Cortex	Neuropil	+	Neuropil	+
Hippocampus	Neurons	−	Pyramidal neurons in CA2-4	++
	Glia	+	Pyramidal neurons in CA1	+
	Neuropil	+	Glia	−
			Neuropil	+
Basal Ganglia	Neurons in subthalamic nucleus and globus pallidus	++	Neurons in subthalamic nucleus and globus pallidus	++
	Neurons in striatum	−	Neurons in striatum	+
	Glial soma	+	Glial soma	−
	Neuropil in striatum	++	Neuropil in striatum	++
	Other nuclei	+	Other nuclei	+
Midbrain	Neurons in substantia nigra and periaqueductal gray	++	Neurons in substantia nigra and periaqueductal gray	++
	Neurons in red nucleus	−	Neurons in red nucleus	+
	Glia	+	Glia	−
Cerebellum	Purkinje cells	−	Purkinje cells	++
	Internal granule neurons	−	Internal granule neurons	+
	Bergman glia	+	Bergman glia	−
	Molecular layer	+	Molecular layer	+

The table lists immunoreactivity for these 2 enzymes in neuron soma, glia soma, or neuropil as absent (−), present (+), or strongly present (++).

was measured with Protein Assay Reagent (BioRad, Hercules, CA) using bovine serum albumin as the standard.

SDS-PAGE

Human brain tissue (frontal cortex or hippocampus) was homogenized in a 10-fold volume of buffer (50 mM hepes, pH 7.0, 4°C) containing PMSF 5 μg/ml. The homogenate was boiled for 10 min and passed through a 28-gauge needle to shear the DNA. Samples were diluted to 0.5 mg/ml in SDS-PAGE sample buffer containing 50 mM dithiothreitol and boiled for 5 min. Electrophoresis was performed on 8%–16% polyacrylamide gradient gels (BioRad) at 160 V for 50 min.

Isoelectric Focusing

Isoelectrofocusing (IEF) gel electrophoresis of sample homogenates was performed using vertical polyacrylamide IEF gels (pH 5–8 or pH 3–10) from BioRad. Homogenates were diluted 4:1 with 50% glycerol containing bromophenol blue. Samples were electrophoresed at 4°C with starting voltage of 100 V for 1 h, followed by 250 V for 1 h, and finally 500 V for 30 min.

Immunoblotting

Following gel electrophoresis (either SDS-PAGE or IEF), proteins were transferred to Sequiblot PVDF membranes (BioRad) at 70 V for 70 min. Membranes were blocked with 3% nonfat dry milk in tris-buffered saline (TBS) for 3 h at room temperature. Antisera were diluted (ALDH 1:20,000; ADH 1:1,000, AKR1A1 1:5,000, AKR1B1 1:5,000) in blocking solution containing 0.2% (vol/vol) tween 20. Membranes were incubated with the antibodies for 16 h at 4°C. The membranes were washed with TBS containing 0.2% (vol/vol) tween 20 (twice for 5 min) followed by TBS (twice for 5 min). Horseradish peroxidase conjugated anti-rabbit secondary antibody (1:2,500, Southern Biotechnology, Birmingham, AL) was incubated with the blots for 2 h at room temperature and washed as above. Blots were developed using chemiluminescent substrate (NEN Life Science Products, Boston, MA) with Kodak BioMax film or a chromogenic substrate (TMB-Blotting; Pierce, Rockford, Il).

Immunohistochemistry

Immunohistochemistry was performed as previously described on 8-μm sections from tissue blocks that had been fixed in formalin and embedded in paraffin using the Trilogy™ antigen retrieval system (Cell Marque, Austin, TX) (6). Primary antisera to ALDH, aldose reductase, aldehyde reductase, and ADH were used at 1:1,000, 1:200, 1:200, and 1:250 dilutions, respectively. Antisera against CD68 (Dako, Carpinteria, CA), GFAP (Dako), and Aβ peptide (Zymed, South San Francisco, CA) were used at a 1:100, 1:1,000, and 1:25 dilutions, respectively. Secondary antibody was conjugated to horseradish peroxidase and diaminobenzidine was used as chromogen substrate. For immunostaining against 2 antigens, 1 secondary antibody was conjugated to alkaline phosphatase with Fast Red used as a substrate. Controls included omission of primary antiserum or competition of primary antiserum with excess purified antigen.

Determination of PMI Effects

Ten-week-old, male, CB57/Bl6 mice (Jackson Labs) were killed by exposure to carbon dioxide. Brains were removed at

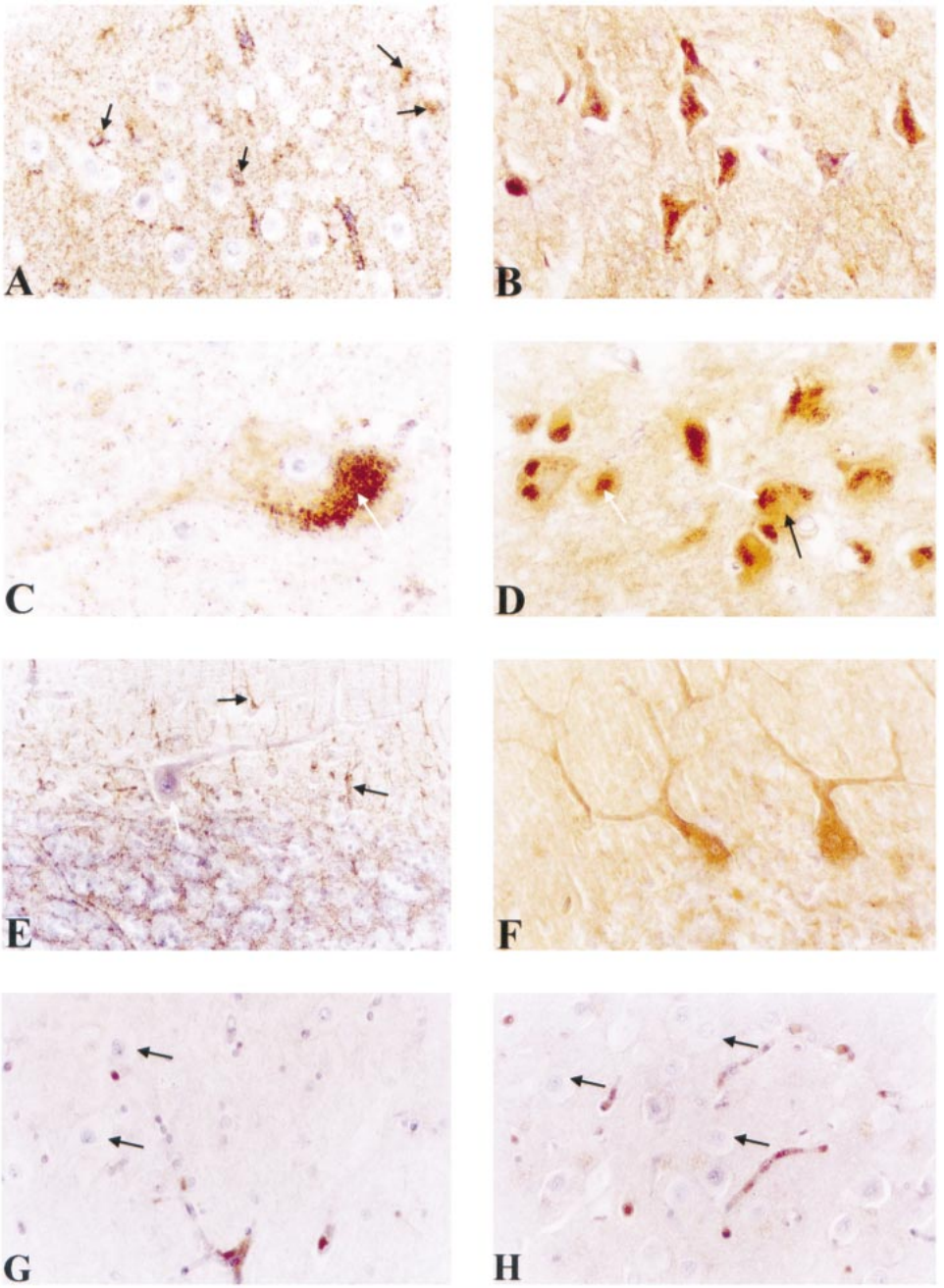

Fig. 2. Localization of ALDH, aldose reductase, aldehyde reductase, and ADH in human brain. ALDH immunoreactivity is noted in glia (black arrows) of the frontal cortex (A), dopaminergic neurons (C) of the substantia nigra (the white arrow denotes neuromelanin), and Bergmann glia (noted by black arrows) of the cerebellum (E). Diffuse, punctate staining was generally observed in the neuropil but was concentrated in glial soma and surrounding blood vessels (A, E). Aldose reductase immunoreactivity was localized to neuronal soma in the frontal cortex (B), dopaminergic neurons (D) of the substantia nigra (white arrows denote neuromelanin, black arrows denote positive immunostaining), and cerebellar Purkinje neurons and internal granule neurons (F). Aldehyde reductase immunoreactivity (G) and ADH immunoreactivity (H) were localized to blood cells in the hippocampus (black arrows denote immunonegative pyramidal neurons). Magnifications: A, B, D–H, ×400; C, ×1,000.

time of death, or 3 or 7 h postmortem and then frozen and stored at −80°C until used.

Aldehyde Oxidoreductase Assays

Frozen samples were weighed and homogenized in a 10-fold volume (weight/volume) of ice-cold isolation buffer (20 mM NaH_2PO_4, pH 7.0 at 4°C) containing 0.1% Triton X-100, 1 mM diethylenetriaminepentaacetic acid (DTPA), and 50 μM butylated hydroxytoluene (BHT). Samples were centrifuged at 14,000 g for 10 min at 4°C to pellet cellular debris and the supernatant retained. Aliquots of the supernatant were frozen for subsequent immunochemical assays.

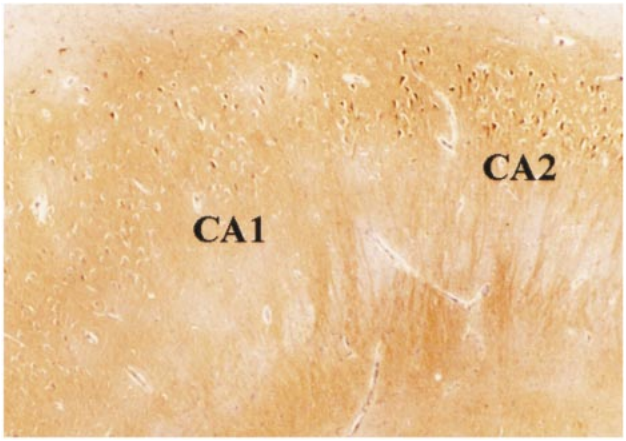

Fig. 3. Lower aldose reductase immunoreactivity in CA1 hippocampal neurons. A section of hippocampus from a control individual probed with anti-aldose reductase antiserum. Note the neuropil immunoreactivity. Aldose reductase immunoreactivity was lower in CA1 pyramidal neurons compared with CA2 pyramidal neurons (×40).

ALDH activity was assayed by measuring the increase in fluorescence of NADH (excitation = 340 nm, emission = 445 nm) in a fluorescent microplate reader (SpectraMax Gemini, Molecular Devices, Sunnyvale, CA) (39). Assay buffer was 0.1 M NaH_2PO_4, pH 7.4, and assays were performed at 37°C. Buffer (240 μl), supernatant (50 μl), and NAD^+ (1 mM, Sigma, St. Louis, MO) were combined and monitored for 10 min until a baseline rate of fluorescence was reached. To measure low K_M ALDH activity (either class 1 or class 2 ALDH), propionaldehyde (70 μM; Sigma) was added and the reaction monitored for 10 min. Low K_M activity was taken to be the propionaldehyde-stimulated rate of fluorescent increase minus the baseline rate with added NAD^+ alone. 1.2 mM propionaldehyde was then added to measure remaining ALDH activity termed high K_M activity (40). High K_M activity was determined by subtracting the total 70 μM propionaldehyde-stimulated rate from the 1.2 mM propionaldehyde-stimulated rate. Protein concentrations of supernatant were determined, and the ALDH activity calculated as nmol NADH formed/min/mg protein. Assays of each sample were performed in quadruplicate and mean rates determined.

Aldose reductase activity was measured in brain homogenates with glyceraldehyde (10 mM) and NADPH (0.1 mM) as substrates using a modified procedure of Song et al in which the formation of $NADP^+$ is measured fluorometrically (41, 42). The use of xylose as a more selective substrate for aldose reductase was not compatible with the fluorometric determination of $NADP^+$ (43). Assays were performed at 37°C. Samples (25 μl) were added to 75 μl assay buffer (50 mM KPO_4, pH 6.6, containing 0.2 M $LiSO_4$) and incubated for 5 min. NADPH was added and the samples incubated for an additional 1 min. The reaction was started by the addition of glyceraldehyde and proceeded for 10 min. The reaction was stopped by the addition of 25 μl of 2N HCl. 6N NaOH (750 μl) containing 10 mM, imidazole was added and the samples heated at 60°C for 10 min and then cooled on ice. 200 μl of this reaction was loaded per well in 96 well plates. Fluorescence was measured using 370 nm excitation and 445 nm emission. Samples were analyzed with and without ethyl 1-benzyl-3-hydroxy-2(5H)-oxopyrrole-4-carboxylate (EBPC, 1 μM), a highly selective inhibitor of aldose reductase (44, 45). EBPC was the kind gift of Pfizer Central Research (Groton, CT). Aldose reductase activity was taken as the EBPC-inhibited rate of fluorescence formation and expressed as nmol NADP+ formed/min/mg protein (45). Assays on each sample were performed in triplicate and mean rates were determined.

Statistical Analyses

Statistical analyses were performed using Prism software (GraphPad, Inc., San Diego, CA) Student *t*-test and analysis of variance were used as needed.

RESULTS

Immunoblots were performed to determine antisera specificity in homogenates of human cerebral cortex and hippocampus; immunoreactive bands of identical molecular weight were obtained from both sites. Antiserum raised against human class 2 ALDH recognized purified class 1 and class 2 ALDH, but not class 3 (Fig. 1A). The 1 immunoreactive band comigrated with purified class 2 ALDH protein (Fig. 1B). Antiserum against human aldose reductase recognized a band that comigrated with purified human aldose reductase (Fig. 1C) (26, 46). A less intense, higher molecular weight aldose reductase-immunoreactive band also was detected; this band has been noted previously by others (26, 46). Competition with purified human aldose reductase ablated signal for both bands. A single immunoreactive band that comigrated with purified aldehyde reductase was present (Fig. 1D). An immunoreactive band was highlighted by anti-ADH antiserum (Fig. 1E) and this was blocked by competition with purified ADH β_1 (not shown).

These antisera were used to localize the aldo-keto oxidoreductases within several regions of brain from control individuals. Omission of primary antiserum was used as negative control in all experiments. In addition, competition with excess purified protein was performed with class 2 ALDH and recombinant aldose reductase; in all cases competition ablated tissue immunoreactivity. Whereas anti-ADH antiserum was reactive with only discrete sites in brain (see below), inclusion of ADH β_1 as competitor led to blanket immunoreactivity with all tissue elements, presumably secondary to nonspecific binding of ADH β_1 to tissue; this precluded competition experiments in tissue for ADH immunoreactivity. Thus, although ADH antiserum reacted with a single band of appropriate mass on immunoblots of cerebral cortex and hippocampus and this was fully competed by ADH β_1, inability to perform competition experiments in tissue limits certainty about the specificity of this antiserum in tissue.

Immunoreactivity for ALDH and aldose reductase was concentrated in gray matter of cerebral cortex, hippocampus, basal ganglia, midbrain, and cerebellum with only scattered immunoreactive cells in white matter. Choroid plexus

epithelium was immunoreactive for both ALDH and aldose reductase; however, neither enzyme was localized to blood vessel walls or leptomeninges. The distribution of ALDH and aldose reductase immunoreactivities in cerebral cortex, hippocampus, basal ganglia, midbrain, and cerebellum is summarized in the Table. In the cerebral cortex and hippocampus, glial cell bodies but not neuron cell bodies displayed punctate ALDH immunoreactivity (Figs. 2A, 5A, B). In addition, neuropil showed diffusely scattered, punctate ALDH immunoreactivity. Double label immunohistochemistry for GFAP or CD68 plus ALDH showed that the vast majority of ALDH-immunoreactive glia were astrocytes although some ALDH glial immunoreactivity colocalized with CD68, a microglial marker (not shown) (47, 48). In contrast, aldose reductase immunoreactivity in the cerebral cortex and hippocampus was localized exclusively to pyramidal neuron cell bodies where it showed diffuse cytoplasmic staining (Fig. 3B). Unlike the intensity of ALDH immunoreactivity that was relatively uniform among cells, pyramidal neurons in the cerebral cortex and hippocampus showed variability in the intensity of aldose reductase immunoreactivity, although virtually every neuron showed at least some immunoreactivity. This variation in the intensity of aldose reductase immunoreactivity was most striking in the hippocampus where pyramidal neurons in CA1 were conspicuously and consistently less immunoreactive than pyramidal neurons in the other hippocampal sectors (Fig. 3).

Punctate glial soma and neuropil immunoreactivity for ALDH was maintained in basal ganglia, midbrain, and cerebellum; however, neurons in the subthalamic nucleus, globus pallidus, substantia nigra, and periaqueductal gray matter also showed ALDH immunoreactivity (Fig. 2C, E). This is not surprising, at least for dopaminergic neurons in the substantia nigra, where ALDH is known to catalyze the terminal step in the synthesis of 3,4-dihydroxyphenylacetic acid (DOPAC). Similar to cerebral cortex and hippocampus, aldose reductase did not localize to glial soma in the basal ganglia, midbrain, or cerebellum; however, neuron cell bodies showed diffuse cytoplasmic immunoreactivity in all of these brain regions (Fig. 2D, F).

Aldehyde reductase was localized to the cytoplasm of cerebellar internal granule cells, choroid plexus epithelium, and blood cells within vessels; however, there was no immunoreactivity with brain parenchyma in the cerebral cortex, basal ganglia, or midbrain (Fig. 2G). ADH was localized to glia in the cerebellum, vascular smooth muscle cells within brain and in the sub-arachnoid space, blood and blood cells within small vessels, and to choroid plexus epithelium (Fig. 2H). There was no nuclear staining with any of the 4 antiserum.

These data indicated that of the 4 aldo-keto oxidoreductases that will detoxify HNE and related aldehydes, only ALDH and aldose reductase were present in cerebral cortex and hippocampus, the regions of brain involved by AD. Isoelectric focusing followed by immunoblotting with anti-ALDH was used to distinguish class 1 ALDH from class 2 ALDH. Only class 2 ALDH was identified in homogenates of superior and middle temporal gyri (SMTG) from controls (n = 6, representative blot shown in Fig. 4). These results are in accord with northern blot data demonstrating only class 2 ALDH mRNA in human brain (30).

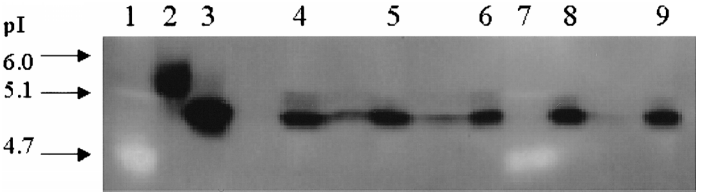

Fig. 4 Mitochondrial class 2 ALDH is the dominant form of ALDH in cerebral cortex. Isoelectric focusing (pH 5–8) of SMTG followed by immunoblotting with anti-class 2 ALDH antibody. Lane 1and 7 = isoelectric point markers, lane 2 = class 1 ALDH (40 ng), lane 3 = class 2 ALDH (40 ng), lanes 4, 5, 6, 8 = homogenate of SMTG from AD brain, lane 9 = homogenate of SMTG from control brain. Note: No difference in class type or migration occurs between ALDH derived from control or AD brain.

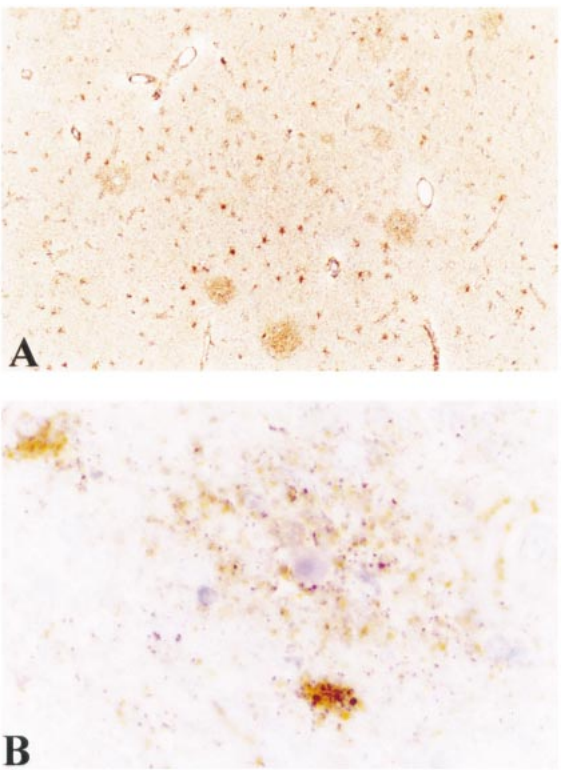

Fig. 5. ALDH immunoreactivity of senile plaques. A: Low power (×40) magnification of a section of frontal cortex from a patient with AD stained with anti-ALDH. ALDH immunoreactivity is elevated in plaque areas. Numerous immunopositive glia are also highlighted. B: High-power magnification (×1,000) of a senile plaque immunoreactive for ALDH. The amyloid core of the plaque is not immunoreactive.

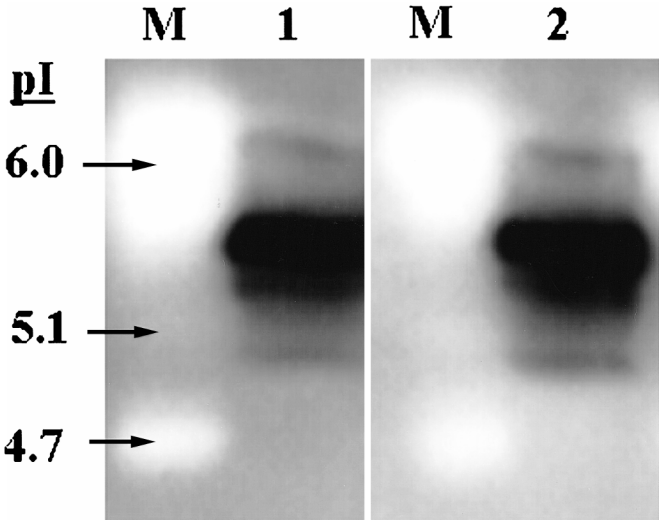

Fig. 6. Biochemical characterization aldose reductase in AD temporal cortex. Isoelectric focusing (pH 3–10) of SMTG homogenates from control (lane 1) or AD brain (lane 2) followed by immunoblotting using anti-aldose reductase antibodies. Isoelectric point protein standards were loaded in lanes marked ''M''. No difference in the isoelectric focussing pattern of aldose reductase was noted.

Next, we tested the hypothesis that alterations in localization, class distribution, or activity of ALDH or aldose reductase may occur in the cerebral cortex and hippocampus of AD patients. ALDH immunoreactive processes were present in senile plaques in cerebral cortex and hippocampus, likely a result of reactive glia within these structures (Fig. 5A, B). Plaque ALDH immunoreactivity colocalized mostly with GFAP but also some with CD68 (not shown). Indeed, ALDH immunoreactivity in AD cerebrum was virtually identical to GFAP immunoreactivity. Double label immunohistochemistry for ALDH and Aβ peptides showed that most plaques possessed ALDH-immunoreactive processes (not shown). ALDH immunoreactivity still was undetectable in cerebral cortical and hippocampal neurons in AD patients. No alteration in the distribution or apparent intensity of aldose reductase was observed in cerebral cortex or hippocampus of AD patients.

Class distribution of ALDH in SMTG of AD patients (n = 4) was identical to controls; only class 2 ALDH was observed (Fig. 4). Although there is only 1 class of aldose reductase in brain, its pI varies with the thiol redox status of the enzyme (46). Therefore, the pI of aldose reductase in SMTG was determined in AD patients and controls (Fig. 6); there was no difference in the pI for aldose reductase between these 2 groups.

Finally, we determined the activity of ALDH and aldose reductase in cerebral cortex from controls and AD patients. In order to determine the effect of PMI on enzyme activity, low K_M (class 1 and class 2) and high K_M ALDH were determined in mouse brain with PMI = 0, 3, or 7 h. Low K_M activity was not significantly altered between 0 h (0.218 ± 0.021 nmol/min/mg; n = 4) and 3 h (0.243 ± 0.029 nmol/min/mg; n = 4). At 7 h postmortem, low K_M ALDH activity was significantly decreased versus 0 and 3 h PMI (0.136 ± 0.013 nmol/min/mg; n = 4; $p < 0.05$). High K_M activity was not altered at 3 or 7 h. Based on these findings, all human tissue used in activity studies had PMI < 3 h. Low K_M but not high K_M ALDH activity was increased in homogenates of SMTG from AD patients compared to controls ($p < 0.05$, Fig. 7A). Combined with the earlier results from isoelectric focusing gels, these data indicate that class 2 ALDH activity is increased in temporal cortex of AD patients. Reductase activity was determined in the same in SMTG samples as used for ALDH activity. Aldose reductase activity was defined as fraction of total reductase activity that was blocked by EBPC, a potent and highly selective inhibitor of aldose reductase. In contrast to low K_M

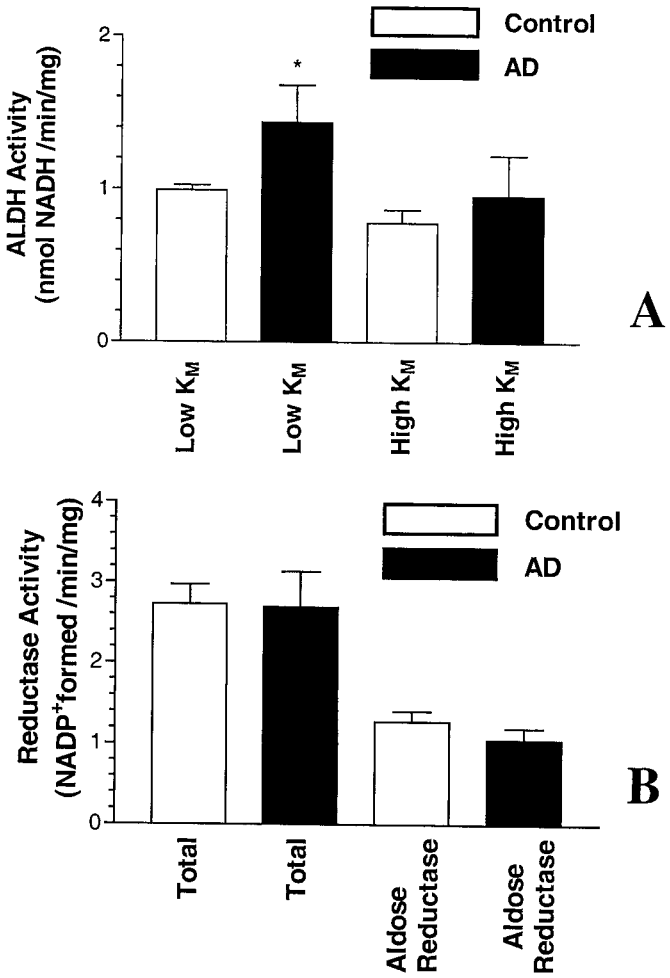

Fig. 7. Low K_M ALDH activity but not aldose reductase activity is elevated in AD. A: ALDH activity was measured using homogenates of the superior middle temporal gyrus from 6 controls and 4 AD patients. B: Total reductase and aldose reductase activity was measured using the identical samples as for the ALDH activity measurements. Aldose reductase activity is defined as the rate of reductase activity inhibited by 1 μM EBPC. * = $p < 0.05$ using the Student *t*-test.

ALDH activity, there was no significant difference in total reductase or aldose reductase activity between AD patients and controls (Fig. 7B).

DISCUSSION

Oxidative stress generates numerous reactive intermediates, and when these exceed the anti-oxidant defenses of the organism, oxidative damage ensues. Thus, increased levels of oxidative stress or decreased anti-oxidant defenses may underlie the regionally increased oxidative damage to brain that is a feature of AD (49, 50). Several detoxification pathways for reactive intermediates produced from oxidative stress have evolved to protect against oxidative damage, these include DNA repair enzymes, superoxide dismutases, catalase, glutathione-dependent enzyme systems, and aldo-keto oxidoreductases (51). All of these except aldo-keto oxidoreductases already have been studied with respect to AD (24, 52–56). This is a potentially important gap in our knowledge because aldo-keto oxidoreductases along with GSTs are the major detoxifying systems for reactive aldehydes such as HNE and acrolein in other organs, and these reactive aldehydes are proposed to be important in AD progression. If this proposal is correct, then aldo-keto oxidoreductase or GST activities in diseased regions of AD brain might be expected to increase in response to reactive aldehyde generation. Contrary to this expectation, others have recently shown that GST activity is decreased in diseased regions of AD brain compared to controls (24).

In the present study, we examined the cellular expression and activities of the major oxidoreductases that metabolize HNE and related aldehydes in brain. We found that mitochondrial class 2 ALDH is the major form in human cerebral cortex and that expression of this enzyme was limited to glia in cerebral cortex and hippocampus. Expression of aldose reductase was complimentary to ALDH; aldose reductase was limited to pyramidal neuron cytoplasm in cerebral cortex and hippocampus. Moreover, pyramidal neuron immunoreactivity for aldose reductase was not uniform. For example, pyramidal neurons in hippocampal sector CA1, a region with heightened vulnerability to a number of injuries, were less immunoreactive for aldose reductase than were pyramidal neurons in other hippocampal sectors. Aldehyde reductase and ADH were not expressed in brain parenchyma of cerebral cortex or hippocampus. Class 2 ALDH immunoreactivity was prominent in senile plaques and low K_M ALDH activity was significantly increased in temporal cortex from AD patients compared with controls. Neither the distribution nor activity of cerebral cortical aldose reductase was different between AD patients and controls. In contrast to GST activity, induction of ALDH activity and expression in senile plaques are consistent with the hypothesis that reactive aldehyde generation is a significant stress to brain in AD.

HNE-protein adducts, acrolein-protein adducts, and protein carbonyls accumulate in AD largely in cerebral cortical and hippocampal neuron cytoplasm with less accumulation in glial cytoplasm (6, 8, 9, 13, 57). Two possible explanations for the preferential accumulation of aldehyde-modified proteins in neurons are either greater lipid peroxidation in neurons than in glia, or less detoxification of reactive aldehydes in neurons than in glia. The former possibility is supported by recent work from our laboratory; diseased regions of AD brain have significantly greater neuroprostanes (free radical oxidation products from docosahexaenoic acid that is concentrated in neurons) than isoprostanes (free radical oxidation products from arachidonic acid that is evenly distributed among brain cells) (58). The fact that aldose reductase has a k_{cat} for HNE that is over 30 times greater than class 2 ALDH does not support the second possibility that neurons are less able to detoxify reactive aldehydes (25, 35). However, our results showed that only ALDH activity was increased in AD brain. Moreover, class 2 ALDH compartmentalization to mitochondria may enhance overall protective function since the majority of oxygen free radicals are thought to derive from mitochondria. Clearly, the issue of relative protection from reactive aldehydes in neurons and glia in vivo is complex and cannot be resolved from these data; nevertheless, our results do show that cerebral cortical and hippocampal neuronal mitochondria lack a major detoxification pathway for reactive aldehydes.

Similar to what we observed with ALDH, increased glial expression of enzymes to detoxify reactive intermediates or pro-oxidants has been observed previously in AD brain. Manganese superoxide dismutase (Mn-SOD) is localized to mitochondria and catalyzes the detoxification of superoxide (54). Heme oxygenase-1 (HO-1) catalyzes the conversion of heme, a pro-oxidant, to compounds with anti-oxidant activity (55, 56). In AD, both Mn-SOD and HO-1 are prominently expressed in reactive astrocytes and both enzymes are localized to senile plaques (54–56). In contrast to ALDH, Mn-SOD and HO-1 are expressed in pyramidal neurons in controls, and HO-1 also is associated with neurofibrillary pathology in AD (56).

Whether elevations in ALDH expression are a direct result of oxidative stress or exposure to reactive aldehydes such as HNE is not known and must be addressed using model systems such as in vitro cell culture. Comparison of ALDH activity with levels of unreacted HNE from postmortem tissue is confounded by the fact that elevations in tissue ALDH activity may lead to a decrease in the tissue levels of HNE through metabolism of HNE to 4-hydroxy-2-nonenoate. Indeed, previous work has shown that tissue levels of unreacted HNE are not significantly elevated in the SMTG of patients with AD even

though other nonmetabolized markers of lipid peroxidation are elevated in the SMTG in AD (59, 60).

The results from our experiments demonstrated that the cellular distribution of the 4 aldo-keto oxidoreductases that metabolize HNE varies among regions of human brain. Especially interesting was ALDH, which was exclusively localized to glia in the cerebral cortex and hippocampus but was present in neurons of some basal ganglia and substantia nigra. Also intriguing was the finding that the cerebellum expressed all 4 of the oxidoreductases investigated. The potential relationship between these differences in distribution of aldo-keto oxidoreductases and the susceptibility of these brain regions to diseases involving oxidative stress remains to be established. While our results agree with the earlier immunohistochemical report on ADH in human brain, our results do not agree with the only previous report on the distribution of aldose reductase in human brain (36). The reasons for these differences are not known; however, it should be noted that this earlier study did not insure specificity of antiserum by performing Western blots on brain homogenates or by competition experiments in tissue sections.

Our results suggest that increased class 2 ALDH activity in cerebral cortex and hippocampus of AD patients is a protective response to increased reactive aldehyde generation in this disease. The significance of class 2 ALDH activity to the progression of AD is further underscored by a recent association between inheritance of a dominant negative inactive allele for class 2 ALDH and increased risk for AD (32). It is noteworthy that ALDH activity can be reduced by a number of dietary and environmental factors in addition to inheritance (32, 61). In combination, these data suggest that mitochondrial ALDH is an important means by which cerebral cortex and hippocampus attempt to limit damage in AD, and may represent a focus where genetic and environmental factors may influence the initiation or progression of AD.

REFERENCES

1. Esterbauer H, Schaur R, Zollner H. Chemistry and biochemistry of 4-hydroxynonenal, malondialdehyde, and related aldehydes. Free Radic Biol Med 1991;11:81–128
2. Witz G. Biological interactions of α,β-unsaturated aldehydes. Free Radic Biol Med 1989;7:333–49
3. Guichardant M, Taibi-Tronche P, Fay L, Lagarde M. Covalent modifications of aminophospholipids by 4-hydroxynonenal. Free Radic Biol Med 1998;25:1049–56
4. Amarnath V, Valentine WM, Montine TJ, et al. Reactions of 4-hydroxy-2(E)-nonenal and related aldehydes with proteins studied by carbon-13 nuclear magnetic resonance spectroscopy. Chem Res Toxicol 1998;11:317–28
5. Sayre LM, Arora PK, Iyer RS, Salomon RG. Pyrrole formation from 4-hydroxynonenal and primary amines. Chem Res Toxicol 1993;6:19–22
6. Montine KS, Kim PJ, Olson SJ, Markesbery WR, Montine TJ. 4-hydroxy-2-nonenal pyrrole adducts in human neurodegenerative disease. J Neuropathol Exp Neurol 1997;56:866–71
7. Montine KS, Olson SJ, Amarnath V, Whetsell WO, Jr.,Graham DG, Montine TJ. Immunohistochemical detection of 4-hydroxy-2-nonenal adducts in Alzheimer's disease is associated with inheritance of APOE4. Am J Pathol 1997;150:437–43
8. Montine KS, Reich E, Neely MD, et al. Distribution of reducible 4-hydroxynonenal adduct immunoreactivity in Alzheimer disease is associated with APOE genotype. J Neuropathol Exp Neurol 1998; 57:415–25
9. Calingasan N, Uchida K, Gibson G. Protein-bound acrolein: A novel marker of oxidative stress in Alzheimer's disease. J Neurochem 1999;72:751–76
10. Lovell MA, Ehmann WD, Mattson MP, Markesbery WR. Elevated 4-hydroxynonenal in ventricular fluid in Alzheimer's disease. Neurobiol Aging 1997;18:457–61
11. Selley M. (E)-4-Hydroxynonenal may be involved in the pathogenesis of Parkinson's disease. Free Radic Biol Med 1998;25:169–74
12. Smith RG, Henry YK, Mattson MP, Appel SH. Presence of 4-hydroxynonenal in cerebrospinal fluid of patients with sporadic amyotrophic lateral sclerosis. Ann Neurol 1998;44:696–69
13. Sayre LM, Zelasko DA, Harris PL, Perry G, Salomon RG, Smith MA. 4-Hydroxynonenal-derived advanced lipid peroxidation end products are increased in Alzheimer's disease. J Neurochem 1997; 68:2092–97
14. Picklo M, Amarnath V, McIntyre J, Graham D, Montine T. 4-Hydroxy-2(E)-nonenal inhibits CNS mitochondrial respiration at multiple sites. J Neurochem 1999;72:1617–24
15. Neely MD, Sidell KR, Graham DG, Montine TJ. The lipid peroxidation product 4-hydroxynonenal inhibits neurite outgrowth, disrupts neuronal microtubules, and modifies cellular tubulin. J Neurochem 1999;72:2323–33
16. Siems W, Hapner S, Kujik Fv. 4-hydroxynonenal inhibits Na+-K+-ATPase. Free Radic Biol Med 1996;20:215–23
17. Keller JN, Mark RJ, Bruce AJ, et al. 4-Hydroxynonenal, an aldehydic product of membrane lipid peroxidation, impairs glutamate transport and mitochondrial function in synaptosomes. Neuroscience 1997;80:685–96
18. Keller JN, Hanni KB, Markesbery WR. 4-hydroxynonenal increases neuronal susceptibility to oxidative stress. J Neurosci Res 1999; 58:823–30
19. Kruman I, Bruce-Keller AJ, Bredesen D, Waeg G, Mattson MP. Evidence that 4-hydroxynonenal mediates oxidative stress-induced neuronal apoptosis. J Neurosci 1997;17:5089–100
20. Mark RJ, Lovell MA, Markesbery WR, Uchida K, Mattson MP. A role for 4-hydroxynonenal, an aldehydic product of lipid peroxidation, in disruption of ion homeostasis and neuronal death induced by amyloid beta-peptide. J Neurochem 1997;68:255–64
21. Mark RJ, Pang Z, Geddes JW, Uchida K, Mattson MP. Amyloid beta-peptide impairs glucose transport in hippocampal and cortical neurons: Involvement of membrane lipid peroxidation. J Neurosci 1997;17:1046–54
22. Hubatsch I, Ridderstrom M, Mannervik B. Human glutathione transferase A4–4: An alpha class enzyme with high catalytic efficiency in the conjugation of 4-hydroxynonenal and other genotoxic products of lipid peroxidation. Biochem J 1998;330:175–79
23. Xie C, Lovell MA, Markesbery WR. Glutathione transferase protects neuronal cultures against four hydroxynonenal toxicity. Free Radic Biol Med 1998;25:979–88
24. Lovell MA, Xie C, Markesbery WR. Decreased glutathione transferase activity in brain and ventricular fluid in Alzheimer's disease. Neurology 1998;51:1562–66
25. Mitchell D, Petersen D. The oxidation of α,β, unsaturated aldehydic products in lipid peroxidation by rat liver aldehyde dehydrogenases. Toxicol Appl Pharmacol 1987;87:403–10
26. O'Connor T, Ireland LS, Harrison DJ, Hayes JD. Major differences exist in the function and tissue-specific expression of human aflatoxin B1 aldehyde reductase and the principal human aldo-keto reductase AKR1 family members. Biochem J 1999;343:487–504

27. Ryzlak M, Pietruszko R. Human brain Glyceraldehyde-3-phosphate dehydrogenase, succinic semialdehyde dehydrogenase and aldehyde dehydrogenase isozymes: Substrate specificity and sensitivity to disulfiram. Alcoholism: Clin Exp Res 1989;13:755–61
28. Lindahl R, Petersen DR. Lipid aldehyde oxidation as a physiological role for class 3 aldehdye dehyrdogenases. Biochem Pharmacol 1991;41:1583–87
29. Ryzlak MT, Pietruszko R. Purification and characterization of aldehyde dehydrogenase from human brain. Arch Biochem Biophys 1987;255:409–18
30. Stewart MJ, Crabb DW. Distribution of messenger RNAs for aldehyde dehydrogenase1, aldehyde dehydrogenase 2, and aldehyde dehydrogenase 5 in human tissues. J Invest Med 1996;44:42–46
31. Maring JA, Dietrich RA, Little R. Partial purification and properties of human brain aldehdye dehydrogenases. J Neurochem 1985;45: 1903–10
32. Kamino K, Nagasaka K, Imagawa M, et al. Deficiency in mitochondrial aldehyde dehydrogenase increases the risk for late-onset Alzheimer's disease in the Japanese population. Biochem Biophys Res Commun 2000;273:192–96
33. Sellin S, Holmquist B, Mannervik B, Vallee B. Oxidation and reduction of 4-hydroxyalkenals catalyzed by isozymes of human alcohol dehydrogenase. Biochemistry 1991;30:2514–18
34. Srivastava S, Chandra A, Wang LF, et al. Metabolism of the lipid peroxidation product, 4-hydroxy-trans-2-nonenal, in isolated perfused rat heart. J Biol Chem 1998;273:10893–10900
35. Srivatava S, Watowich SJ, Petrash JM, Srivatava SK, Bhatanagar A. Structural and kinetic determinants of aldehyde reduction by aldose reductase. Biochemistry 1999;38:42–54
36. Wirth HP, Wermuth B. Immunohistochemical localisation of aldehyde and aldose reductase in human tissues. Enzymology of carbonyl metabolism 2.Alan R. Liss, 1985:231–39
37. Mori O, Haseba T, Kameyama K, et al. Histological distribution of class III alcohol dehydrogenase in human brain. Brain Res 2000; 852:186–90
38. Mira SS, Heyman A, McKeel D, et al. The consortium to establish a registry for Alzheimer's disease (CERAD). Part II. Standardization of the neuropatholic assessment of Alzheimer's disease. Neurology 1991;41:479–86
39. Neslon AN, Lipsky JJ. Microtiter plate-based determination of multiple concentration-inhibition relationships. Anal Biochem 1995; 231:437–39
40. Weiner H, Ardelt B. Distribution and properties of aldehdye dehydrogenase in regions of rat brain. J Neurochem 1984;42:109–15
41. Song HP, Das B, Srivastava SK. Microdetermination of aldose and aldehyde reductase from human tissue. Eye Res 1987;6:1001–6
42. Lowry OH, Carter JG. Stabilizating the alkali-generated fluorescent derivatives of NAD and NADP. Anal Biochem 1974;59:639–42
43. Poulsom R. Inhibition of hexonate dehydrogenase and aldose reductase from bovine retina by sorbinil, statil, M79175 and valproate. Biochem Pharmacol 1986;35:2955–59
44. Mylari BL, Beyer TA, Siegel TW. A highly specific aldose reductase inhibitor, ethyl 1-benzyl-3 hydroxy-2(5H)-oxopyrrole-4-carboxylate, and its congeners. J Med Chem 1991;34:1011–18
45. Spycher S, Tabataba-Vakili S, O'Donnell VB, Palomba L, Azzi A. 4-hydroxy-2,3-trans-nonenal induces transcription and expression of aldose reductase. Biochem Biophys Res Commun 1996;226: 512–16
46. Wermuth B, Burgisser H, Bohren K, von Wartburg JP. Purification and characterization of human-brain aldose reductase. Eur J Biochem 1982;127:279–84
47. Andjelkovic AV, Nikolic B, Pachter JS, Zecevic N. Macrophages/microglial cells in human central nervous system during development: An immunohistochemical study. Brain Res 1998;814:13–25
48. Reynolds WF, Rhees J, Maciejewski D, et al. Myeloperoxidase polymorphism is associated with gender specific risk for Alzheimer's disease. Exp Neurol 1999;155:31–41
49. Markesbery WR. Oxidative stress hypothesis in Alzheimer's disease. Free Radic Biol Med 1997;23:134–47
50. Markesbery W, Lovell M. Four-hydroxynonenal, a product of lipid peroxidation, is increased in the brain in Alzheimer's disease. Neurobiol Aging 1998;19:33–36
51. Hayes JD, McLellan LI. Glutathione and glutathione-dependent enzymes represent a co-ordinately regulated defence against oxidative stress. Free Radic Res 1999;31:273–300
52. Lovell MA, Xie C, Gabbita SP, Markesbery WR. Decreased thioredoxin and increased thioredoxin reductase levels in Alzheimer's disease brain. Free Radic Biol Med 2000;28:418–27
53. Lovell MA, Xie C, Markesbery WR. Decreased base excision repair and increased helicase activity in Alzheimer's disease brain. Brain Res 2000;855:116–23
54. Furuta A, Price DL, Pardo CA, et al. Localization of superoxide dismutases in Alzheimer's disease and Down's syndrome neocortex and hippocampus. Am J Pathol 1995;146:357–67
55. Schipper HM, Cisse S, Stopa EG. Expression of heme oxygenase-1 in the senescent and Alzheimer-diseased brain. Ann Neurol 1995; 37:758–68
56. Smith MA, Kutty RK, Richey PL, et al. Heme oxygenase-1 is associated with the neurofibrillary pathology of Alzheimer's disease. Am J Pathol 1994;145:42–47
57. Smith MA, Sayre LM, Anderson VE, et al. Cytochemical demonstration of oxidative damage in Alzheimer disease by immunochemical enhancement of the carbonyl reaction with 2,4-dinitrophenylhydrazine. J Histochem Cytochem 1998;46:731–35
58. Reich EE, Zackert WE, Brame CJ, et al. Formation of novel D-ring and E-ring isoprostane-like compounds (D4/E4-neuroprostanes) in vivo from docosahexaenoic acid. Biochemistry 2000;39: 2376–83
59. Markesbery WR, Lovell MA. Four-hydroxynonenal, a product of lipid peroxidation, is increased in the brain in Alzheimer's disease. Neurobiol. Aging 1998;19:33–36
60. Reich EE, Markesbery WR, Roberts II LJ, Swift LL, Morrow JD, Montine TJ. Brain regional quantification of F-ring and D-/E-ring isoprostanes and neuroprostanes in Alzheimer's disease. Am J Pathol 2001;158:293–97
61. Staub RE, Sparks SE, Quistad GB, Casida JE. S-methylation as a bioactivation mechanism for mono- and dithiocarbamate pesticides as aldehyde dehydrogenase inhibitors. Chem Res Toxicol 1995;8: 1063–69.

Received December 7, 2000
Revision received February 26, 2001
Accepted April 4, 2001